http://dx.doi.org/10.17159/2411-9717/2018/v118n7a3

Investigation of secondary zinc oxides as an alternative feed to the Skorpion Zinc process: Part 1 – leaching alternative zinc oxides

by C. Lottering*† and C. Dorfling†

Synopsis

Skorpion Zinc processes zinc oxide ore using a sulphuric acid leaching, solvent extraction, and electrowinning process to produce Special High Grade zinc. The company investigated the possibility of supplementing ore with alternative zinc oxide sources to extend the life of mine and maximize zinc production. In part 1 of this two-part communication we report on experimental investigations to assess the technical feasibility of recovering zinc from electric arc furnace (EAF) dust, zinc dross, and zinc fume under the current Skorpion Zinc leaching conditions. The metal dissolution and acid consumption were determined at temperatures between 40 and 70°C and pH values between 1.2 and 2.1 for slurries containing 20% solids.

With the current Skorpion Zinc operating conditions of 50°C and pH 1.8, zinc dissolution from the EAF dust, zinc dross, and zinc fume was 93, 96.9, and 98.5 %, respectively. The rate of zinc leaching from dross and from zinc fume decreased as the pH was increased to 1.5 and 1.8, respectively. The rate-determining step for zinc leaching from zinc dross gradually changed with an increase in pH from porous layer mass transport to chemical reaction and/or boundary layer mass transport. In the case of EAF dust, increasing the temperature to 70°C significantly reduced the zinc leaching rate due to the precipitation of calcium sulphate, which inhibited the zinc leaching reactions. The overall acid consumptions for all three alternative oxides investigated were below the current target consumption of 1.5 t acid per ton of Zn in the feed. It would be technically feasible to use EAF dust, zinc dross, and/or zinc fume as supplementary feed to the Skorpion Zinc process.

Keywords
hydrometallurgy, leaching, secondary zinc oxides.

Introduction

Background and objectives

Skorpion Zinc is located in the southwestern Sperrgebiet region in Namibia; it is one of the few mines in the world with an economically viable oxide zinc deposit. The ore is processed in a sulphuric acid leaching circuit under atmospheric conditions, followed by solvent extraction and electrowinning. Zinc casting is finally used to produce 99.995% Special High Grade zinc as final product.

As the orebody is becoming depleted, it becomes increasingly difficult to maintain the targeted production. Skorpion Zinc has investigated several options to ensure that the targeted production levels can be maintained until mine closure despite the declining ore resource. One option involves supplementing the remaining Skorpion Zinc ore with secondary zinc oxides such as electric arc furnace (EAF) dust, galvanizer dross, and natural-state zinc oxide to maintain the plant feed grade and production rate.

The existing plant has been optimized for processing of Skorpion Zinc ore, which differs from alternative zinc oxides in terms of composition and elemental matrices. This study therefore aimed to evaluate the feasibility of supplementing the feed to the Skorpion Zinc plant with alternative zinc oxides. The main objectives were threefold: firstly, to assess whether it is technically feasible to process alternative zinc oxides at the current Skorpion Zinc plant operating conditions; secondly, to determine the maximum amount of different alternative zinc oxides that could be fed to the plant considering operational limitations; and thirdly, to perform an economic analysis to identify the most profitable manner in which to manage supplementation of ore with alternative zinc oxide sources.

Part 1 of this communication deals with the first objective. Here, we report the results of laboratory leaching tests to investigate the effect of key operating conditions on the leaching of zinc and impurities from EAF dust, galvanizer dross, and natural-state zinc oxide. These test results were used subsequently to address the second and third objectives, which are discussed in Part 2 of this communication.

Skorpion Zinc leaching conditions

The Skorpion Zinc process consists of three major steps, namely atmospheric leaching, solvent extraction, and electrowinning. Of primary interest for the first part of the study is the atmospheric leaching stage, which treats ore that has been crushed and milled to 80%

* *Skorpion Zinc Mine, Rosh Pinah, Namibia.*
† *Department of Process Engineering, University of Stellenbosch, South Africa.*

 ISSN 2225-6253. Paper received May 2017; revised paper received Sep. 2017.

passing 180 µm. The leaching section consists of five agitated tanks in series with a total residence time of 2 hours. Sulphuric acid is used as lixiviant at 50°C and pH 1.8–2 in the final leaching tank. A detailed process description is provided in Part 2 of this communication. The main leaching reactions are shown by Equations [1–3] (Gnoinski, 2007).

$$ZnO \cdot SiO_2 + H_2SO_4 + H_2O \rightarrow ZnSO_4 + H_4SiO_4 \quad [1]$$

$$Zn_2SiO_4 + 2H_2SO_4 \rightarrow 2ZnSO_4 + Si(OH)_4 \quad [2]$$

$$Zn_4Si_2O_7(OH)_2 \cdot H_2O + 4H_2SO_4 \rightarrow 4ZnSO_4 + 2Si(OH)_4 + 2H_2O \quad [3]$$

Alternative zinc oxide sources

Electric arc furnace dust

Many steel producers utilize steel scrap as a source of iron. During melting of the steel scrap, volatile components fume off and form vapour, which is then condensed as a fine dust in the off-gas cleaning system (Barrett, Nenniger, and Dziewinski, 1992). With much of the steel scrap sourced from galvanized steel, zinc is one of the major components of the EAF dust; it is typically present in concentrations between 7 and 40% (Pereira *et al.*, 2007).

During the smelting process, many of the zinc compounds contained in the recycled steel are oxidized to form various zinc oxides. However, due to the large amount of iron in the system, some of the zinc is also transformed into zinc ferrites (Jandová, Prošek, and Maixner, 1999). Zinc in the EAF dust is therefore present mainly in the form of zincite (ZnO) or franklinite ($ZnFe_2O_4$), while iron is mainly in the form of magnetite (Fe_3O_4) or haematite (Fe_2O_3). Zinc may also be present as complex ferrites, for example $(ZnMnFe)_2O_4$. Trace elements may occur in the form of franklinite with isomorphously substituted metals, $(Zn_x,A_y)Fe_2O_4$, where A refers to other metals such as manganese, cobalt, calcium, and nickel (Havlik, Friedrich, and Stopic, 2004).

While ZnO is leached with relative ease in both acid and alkaline leaching systems, zinc ferrite is relatively refractory and requires either a more concentrated medium or higher temperatures to be extracted. This could cause co-extraction of iron in the leaching process (Langová, Riplová, and Vallová, 2007; Oustadakis *et al.*, 2010). Zinc is found mainly in the fines in EAF dusts. Here, the zinc is likely to be present in the form of zincite. Zinc and iron in the coarser particles would be predominantly in the form of franklinite (Oustadakis *et al.*, 2010).

Galvanizer dross

During the hot dip galvanizing process, zinc is molten in a bath. The surface of the molten zinc metal is exposed to the atmosphere and reacts with oxygen, forming an oxidized zinc layer. This top dross must occasionally be removed to ensure good galvanizing coatings. Zinc dross also forms at the bottom of the zinc bath by intermetallic reactions that take place within the molten zinc, as well as by entrapment of foreign particles in the molten metal (Trpčevská *et al.*, 2010). Due to the lower purity of the dross, it cannot be recycled directly to the furnaces for recovery, and it is therefore often treated by alternative processes.

Galvanizer dross typically consists of metallic zinc, zinc oxide, zinc chloride, some copper, iron, lead, aluminium, and other impurity elements in both oxide and metallic forms (Behnajady, Babaeidehkordi and Moghaddam, 2014; Dvořák and Jandová, 2005; Shitov *et al.*, 2005). The majority of the metallic zinc typically reports to the coarser size fractions, while the fine size fractions normally contain the oxidized metals and a larger fraction of inclusions (Rabah and El-Sayed, 1995).

Zinc oxide from smelting furnace fumes

Zinc oxide can be collected as a waste product from lead and zinc smelters. These fuming-furnace zinc oxide powders typically contain large amounts of zinc and lead, along with some other metals such as aluminium and cadmium. As previously mentioned, ZnO is easy to leach at moderate temperature and pH conditions. Contaminated sources of zinc oxide generally contain a spinel in addition to the zinc oxides, in which some of the zinc particles are bound. This spinel, which can be represented as $Mn_{1-x}(Zn, Mg, Ni)_x(Al,Cr)_2O_4$, is insoluble and results in incomplete zinc dissolution (Jandová *et al.*, 1999). These zinc oxides also normally contain large quantities of chlorides and fluorides, which can cause downstream processing issues (Li *et al.*, 2015).

Leaching of alternative zinc oxides

Various studies have investigated the effects of operating variables such as temperature, particle size distribution, acid concentration, agitation rate, pH, solids content, residence time, and mineralogy on the leaching of metals from secondary zinc oxides (Cruells, Roca, and Nunez, 1992; Dvořák and Jandová, 2005; Elgersma *et al.*, 1992; Havlík *et al.*, 2006, 2005; Herrero *et al.*, 2010; Hoang Trung, Havlík, and Miškufová, 2015; Jandová *et al.*, 1999; Jha, Kumar, and Singh, 2001; Langová *et al.*, 2007; Moradi and Monhemius, 2011; Oustadakis *et al.*, 2010; Pecina *et al.*, 2008; Rabah and El-Sayed, 1995; Ruşen, Sunkar, and Topkaya, 2008; Shawabkeh, 2010). In general, the effects of the different process variables depended on the composition of the secondary zinc oxides as well as the range of conditions investigated. In this study, secondary zinc oxides were obtained from suppliers that would be considered favourably for supplying material in bulk to the Skorpion Zinc processing plant. The processing conditions for the alternative zinc oxides were furthermore governed by the typical operating conditions currently employed by Skorpion Zinc for ore leaching.

Zn oxides such as zincite tend to dissolve with relative ease according to Equation [4] (Havlik *et al.*, 2004). Zinc ferrite, which is more difficult to dissolve, reacts with sulphuric acid to form zinc sulphate and ferric sulphate, according to Equation [5] (Turan, Altundoğan, and Tümen, 2004), Equation [6] (Havlik *et al.*, 2004), or Equation [7] (Havlík *et al.*, 2006). According to Havlik *et al.* (2004) and Hoang Trung, Havlik, and Miškufová (2015), Equation [5] takes place preferentially over Equations [6] and [7] for the leaching of zinc ferrite in the temperature range from 25°C to 100°C. This reaction has slow kinetics at low temperature and

the reaction rate increases significantly with temperature (Havlik *et al.*, 2004).

$$ZnO + H_2SO_4 \rightarrow ZnSO_4 + H_2O \quad [4]$$

$$ZnFe_2O_4 + 4H_2SO_4 \rightarrow ZnSO_4 + Fe_2(SO_4)_3 + 4H_2O \quad [5]$$

$$ZnFe_2O_4 + H_2SO_4 \rightarrow ZnSO_4 + Fe_2O_3 + H_2O \quad [6]$$

$$ZnFe_2O_4 + H_2SO_4 + H_2O \rightarrow ZnSO_4 + 2Fe(OH)_3 \quad [7]$$

While Montenegro *et al.* (2013) reported that dissolution of iron species is slow at sulphuric acid concentrations below 1 M, magnetite and haematite are leached readily with sulphuric acid under the experimental conditions considered for zinc ferrite leaching. The reaction of haematite with sulphuric acid is shown in Equation [8] (Turan *et al.*, 2004); magnetite leaching with sulphuric acid proceeds according to Equation [9] (Cruells *et al.*, 1992), or Equation [10] in the presence of atmospheric oxygen (Kukurugya, Vindt, and Havlik, 2015).

$$Fe_2O_3 + 3H_2SO_4 \rightarrow Fe_2(SO_4)_3 + 3H_2O \quad [8]$$

$$Fe_3O_4 + 4H_2SO_4 \rightarrow FeSO_4 + Fe_2(SO_4)_3 + 4H_2O \quad [9]$$

$$4Fe_3O_4 + 18H_2SO_4 + O_2 \rightarrow 6Fe_2(SO_4)_3 + 18H_2O \quad [10]$$

Calcium sulphate formed by the reaction of calcium with sulphuric acid is sparingly soluble and is therefore mostly removed with the solid residue. Gangue acid consumption will be affected by all elements in the secondary oxide other than zinc, and could contribute significantly to the total acid consumption in the Skorpion Zinc refinery.

Experimental

Materials

Factors that were considered when selecting potential suppliers of alternative zinc oxides included their location, cost of the material, pre-processing requirements, and zinc concentration and impurity content of the material. The three different materials that were selected as potentially economically feasible supplementary feed to the Skorpion Zinc process included an EAF dust, zinc dross from a hot-dip galvanizer, and zinc oxide produced from the furnace fumes of a zinc smelter. A summary of the elemental compositions of the alternative zinc oxides tested in this project is presented in Table I. All materials were dried in an oven at 50°C until no further change in mass was recorded, and then sieved and pulverized for the leaching tests.

The different alternative zinc oxides had different particle size distributions. The material as received from each supplier was classified as the coarse size fraction. A normal size fraction was prepared for each of the materials by sieving a portion of the material to –180 µm, which is the typical particle size requirement for the current Skorpion Zinc operation. The oversized material was then pulverized for 10 seconds and the process repeated until 80% of the material had a top size of 180 µm. A third size class, the fine fraction, was obtained by pulverizing a portion of the as-received material until all material had a 180 µm top size in the case of EAF dust and zinc fume. For zinc dross, aggregation of zinc particles prevented reduction of all particles to smaller than 180 µm and the milling time was selected based on the EAF dust and zinc fume milling times instead. Particle size distributions were determined by a combination of wet screening and laser diffraction utilizing a Malvern particle size analyser. Synthetic leach solution was prepared for all leaching tests using zinc sulphate heptahydrate, analytical grade sulphuric acid, and demineralized water.

Equipment and procedure

All leaching experiments were conducted using the standard Skorpion Zinc leach test procedure to ensure that the results were comparable with plant tests performed previously. The experiments were performed in a 5 L tall form glass beaker of even diameter equipped with a variable-speed overhead agitator and 50 mm four-blade impeller for mixing. 500 mL demineralized water was placed in the leaching vessel, and the vessel placed in a temperature-controlled water bath. The overhead stirrer was switched on at the desired agitation rate, and the solids were then added to the water and the slurry was allowed to heat to the set-point temperature. Synthetic leach solution resembling the plant raffinate solution and containing 70 g/L sulphuric acid was then added to the slurry to achieve the desired pH for leaching. The pH of the leach solution was measured using a handheld Mettler Toledo pH meter and controlled manually through the addition of 500 g/L sulphuric acid from a burette above the leaching vessel.

Slurry samples were taken every 10 minutes during the first 75 minutes of leaching, and every 20 minutes thereafter for a total leaching time of 135 minutes. These samples were filtered using 0.45 µm syringe filters and the liquid submitted for full elemental analysis by inductively coupled plasma atomic emission spectroscopy (ICP-AES) as well as free acid analysis by titration. Upon completion of each experiment,

Table I

Elemental composition of alternative zinc oxides (%)

	Zn	Fe	Al	Ca	Cu	Ni	Si	Mn	Mg
EAF dust	30	13	1.5	2.5	0.20	0.02	1.8	1.0	1.3
Zn dross	60	2.5	6.6	1.0	0.10	0.15	0.90	0.10	0.17
Zn fume	78	0.70	0.10	0.15	0.15	0.00	1.7	0.06	0.01

the bulk slurry was filtered through a vacuum press and then washed with a heated pH 2 solution to remove any remaining dissolved zinc. The filtrate and the solid residue were submitted for elemental analysis; solid samples were acid-digested and the resulting solutions also analysed using ICP-AES. These analytical results were used to perform mass balance accounting.

Experimental design

The effects of agitation speed and particle size distribution (PSD) on the leaching behaviour were evaluated independently in tests performed using a slurry containing 20% solids (normal size class) at 50°C and pH 1.8. The agitation speed was varied between 500 and 700 r/min to determine the agitation speed required to eliminate the effect of boundary layer mass transfer on the zinc dissolution kinetics. For each of the alternative zinc oxide materials, three samples with qualitatively different particle size distributions (*i.e.* fine, normal, and coarse) were prepared as described above to investigate the effect of the PSD on the leaching behaviour. Subsequently, the effects of leaching temperature and pH on the leaching behaviour of the different alternative zinc sources were evaluated according to a full factorial experimental design. Temperatures of 40, 50, 60, and 70°C and pH values of 1.2, 1.6, 1.8, and 2.1 were investigated for a slurry containing 20% solids in the normal size class. Other operating conditions such as residence time were selected based on the current Skorpion Zinc processing conditions and plant limitations.

Results and discussion

Effect of agitation speed

The effect of agitation on zinc leaching rate was investigated to determine the agitation speed required to prevent mass transport in the boundary layer from limiting the zinc leaching reactions in the experimental set-up. Increasing the agitation rate from 500 r/min to 700 r/min had an insignificant effect on the rate of zinc dissolution and the extent of zinc leaching achieved after 135 minutes, as shown in Figure 1. An agitation rate of 700 r/min was used in all subsequent tests. The differences in rate and extent of zinc leaching observed for the difference alternative zinc sources are discussed later.

Effect of PSD

The PSDs for the different size classes in Table II indicate differences in the breakage behaviour of the different zinc oxide materials. In the case of zinc dross, the fine sample (prepared by pulverizing all material) had a wider size distribution than the normal size distribution (prepared by pulverizing the particles larger than 180 µm). The zinc dross contained a large fraction of metallic zinc. The perceived increase in the particle size with increased pulverization might have been due to metallic particles in the dross being flattened rather than shredded or ground during pulverizing. The finer dust component of the dross furthermore contained small metallic particles which could have undergone aggregation during pulverization.

As expected, the particle sizes decreased during leaching. Reduction in the size of particles in the larger size fractions in some instances resulted in increased 10% and 50% passing sizes. The most significant size reduction was observed for the normal size class zinc dross and the fine and normal size classes of zinc fume, resulting in P_{80} particle sizes of 13 µm or less.

The dissolution of zinc in the different size classes for the respective alternative zinc oxides is shown in Figure 2. While the rate and extent of zinc leaching from the fine and the normal size fractions of zinc fume were comparable, the rate and extent were significantly higher than for the coarse size fraction. The faster leaching rate observed for the smaller particles can be ascribed to the larger specific surface area available for the leaching reactions to proceed. The lower extent of leaching observed for the coarse fraction may be

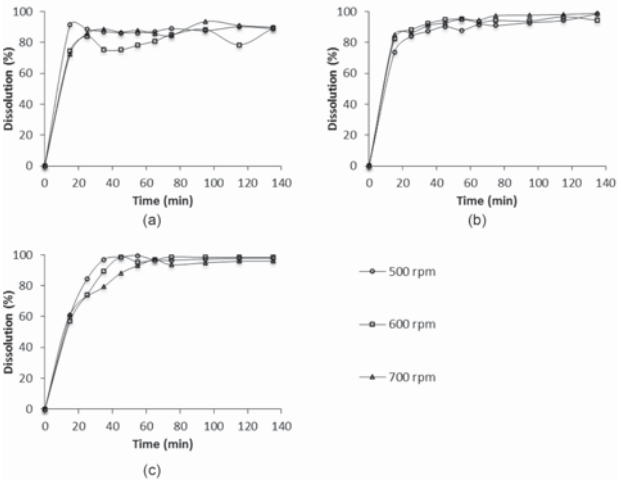

Figure 1—Effect of agitation rate on the rate of zinc leaching from (a) EAF dust, (b) zinc fume, and (c) zinc dross at 50°C and pH 1.8, with slurry containing 20% solids in the normal size fraction

Table II

Particle size distributions for the different size classes of the alternative zinc oxide materials before and after leaching

Material	Size class	P_{10} (µm)	P_{50} (µm)	P_{80} (µm)	P_{90} (µm)
EAF dust (before leaching)	Coarse	1	24	379	671
	Normal	2	41	264	465
	Fine	1	3	38	87
Zn dross (before leaching)	Coarse	11	209	586	851
	Normal	4	72	172	242
	Fine	5	151	391	550
Zn fume (before leaching)	Coarse	9	603	1074	1336
	Normal	1	22	193	256
	Fine	1	8	101	232
EAF dust (after leaching)	Coarse	2	44	239	408
	Normal	1	7	101	249
	Fine	1	4	28	62
Zn dross (after leaching)	Coarse	17	191	446	642
	Normal	1	3	7	31
	Fine	2	39	190	320
Zn fume (after leaching)	Coarse	1	105	393	618
	Normal	1	3	13	60
	Fine	1	3	8	37

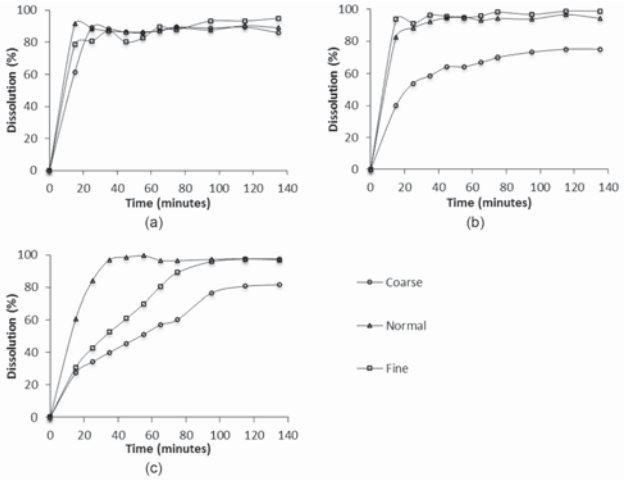

Figure 2—Effect of particle size distribution on the rate of zinc leaching from (a) EAF dust, (b) zinc fume, and (c) zinc dross at 50°C and pH 1.8, with slurry containing 20% solids

due to the entrapment of ZnO in insoluble impurity substances such as spinel phases. After leaching, the P_{80} particle size of 393 µm for the coarse fraction was 30 to 50 times larger than the P_{80} particle sizes for the other size classes.

Considering that the normal size class of the zinc dross had a smaller particle size distribution than the fine class, the results shown in Figure 2c agree with results presented by Moradi and Monhemius (2011); as was the case for the zinc fume samples, decreasing the particle size resulted in faster zinc leaching. The greater difference in the zinc dissolution between the fine size class and the normal size class for zinc dross, compared to zinc fume, can be ascribed to the larger difference in the particle size distributions of the different size classes for the respective materials. It is also noticeable that the zinc leaching rates from the fine and the normal size classes of zinc dross are slower than from same size classes of zinc fume, presumably due to the larger particle size distributions as well as the aggregation of fine metallic particles during pulverization, which decreased the specific surface area of the material and hence the expected leaching rate.

In the case of EAF dust, leaching of zinc from the coarse size fraction proceeded at a faster rate than in the case of zinc fume and zinc dross because of the smaller particles present in the EAF dust coarse fraction. This also suggested that the large particles leached readily under the conditions investigated. Although the initial leaching rate was slightly slower than for the fine and normal size classes, 89% zinc dissolution was achieved after 25 minutes. Zinc dissolution from the normal and coarse size fractions reached equilibrium after 25 minutes, after which there was no significant change in the eluate zinc concentration. For fine particles, zinc dissolution increased gradually from 80% after 25 minutes to 95% after 135 minutes, resulting in a slightly higher overall zinc dissolution compared to the normal and coarse size classes.

Although there was an increase in iron dissolution over this time period (refer to Figure 3), the amount of iron dissolved was stoichiometrically less than what would be expected if the zinc leaching during this period was due solely to zinc ferrite dissolution. This suggested that a portion of the zinc species was either entrapped in insoluble phases or coated with an inert product layer which formed during the initial leaching period. Dissolution of these zinc species was possible only in the fine size class, where the diffusion path through the insoluble phases was sufficiently short for leaching of the zinc species to occur within the time period investigated. The slow zinc leaching rate from 25 minutes to 135 minutes confirmed that a different mechanism (*e.g.* diffusion through insoluble layers) controlled the leaching rate. Had the effect been due purely to improved liberation, the liberated zinc would have likely dissolved at a rate comparable to the rate observed in the first 25 minutes.

Trends in aluminium dissolution generally followed those for zinc leaching; 45–66% aluminium leaching was achieved for zinc dross, and 30–50 % and 35–55% for EAF dust and zinc fume, respectively. The highest iron dissolution of 84% was observed for the normal size class zinc dross, as shown in Figure 3. Iron dissolution was the lowest for EAF dust, ranging between 17 and 21%. Given the relatively high zinc recoveries, the undissolved iron could not be in the form of zinc ferrite or zinc-containing spinel phases; iron was therefore likely to be present mainly as stable oxide phases in the EAF dust, which could inhibit dissolution of entrapped zinc species. Leaching of the zinc fume sample resulted in 35–58% iron dissolution. As was the case for the other materials, the iron concentration increased gradually between 25 minutes and 135 minutes without reaching equilibrium in this time period. The distribution of iron between zinc ferrite and the slow-leaching iron oxide species determined the overall iron dissolution.

Effect of temperature and pH

Zinc leaching

The effect of temperature on the extent of zinc dissolution from zinc fume after 135 minutes was negligible at pH 1.2,

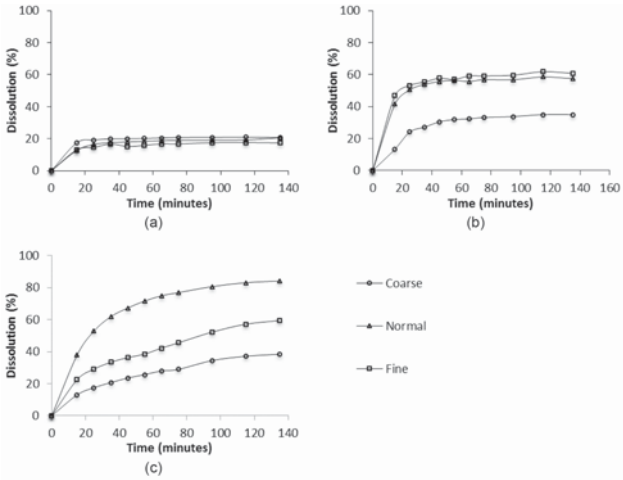

Figure 3—Effect of particle size distribution on the rate of iron leaching from (a) EAF dust, (b) zinc fume, and (c) zinc dross at 50°C and pH 1.8, with slurry containing 20% solids

but increased with an increase in pH. Figure 4 shows that the zinc leaching extent at pH 1.2 varied between 98.4 and 99.6% at 40°C and 70°C, respectively. At pH 2.1, the corresponding zinc leaching percentages were 94.1 and 99.6%, respectively. The effect of pH on the extent of zinc dissolution after 135 minutes was again significant only at the lower temperatures, and was statistically less significant than the effect of the temperature.

For tests conducted at 40°C and 50°C, the initial rate of zinc leaching generally decreased with an increase in pH, particularly at pH values of 1.8 or higher. Although the leaching rates at 60°C for pH 1.5 and pH 1.8 are slow compared to the leaching rates observed at the other conditions, no reasons can be assigned for this behaviour. Overall, it did not appear as if the temperature had a significant effect on the rate of leaching, which suggested that these reactions were mass-transfer limited.

The effect of temperature on zinc dissolution from dross at different pH values is shown in Figure 5. In general, the rate of zinc leaching from dross decreased with increasing pH due to the lower hydrogen ion concentration. At pH 1.5 and pH 1.8, the zinc leaching rate increased with increasing temperature. At pH 1.2 and pH 2.1, however, no clear trend in the leaching rate with temperature was observed. This suggests that the rate-determining mechanism changed with a change in acid concentration, with chemical reaction rate-limiting conditions dominating in the intermediate pH range.

This hypothesis was investigated further by fitting three common leaching mechanism models to the data from the zinc dross leaching experiments conducted at 60°C. The leaching rates during the first 45 minutes are presented in Figure 6. Q represents the leaching models as reported by Prosser (1996) and shown on the left-hand side of Equations [11] to [13]; Equation [11] is the model if mass transport in the boundary layer is the rate-determining step, while Equations [12] and [13] represent the surface chemical reaction-limiting and the mass transport in porous product layer-limiting models, respectively. X refers to the fractional dissolution at time t, and k is the corresponding rate constant.

$$1-(1-X)^{2/3}=kt \quad [11]$$

$$1-(1-X)^{1/3}=kt \quad [12]$$

$$1-\frac{2}{3}X-(1-X)^{2/3}=kt \quad [13]$$

The coefficients of determination (R^2) for the different models in the respective cases are shown in Table III. At pH 1.2, the porous layer mass transport model clearly fitted the data the best; with an increase in pH, a gradual shift from porous layer mass transport-limited leaching to combination of chemical reaction- and boundary layer diffusion-limited leaching occurred.

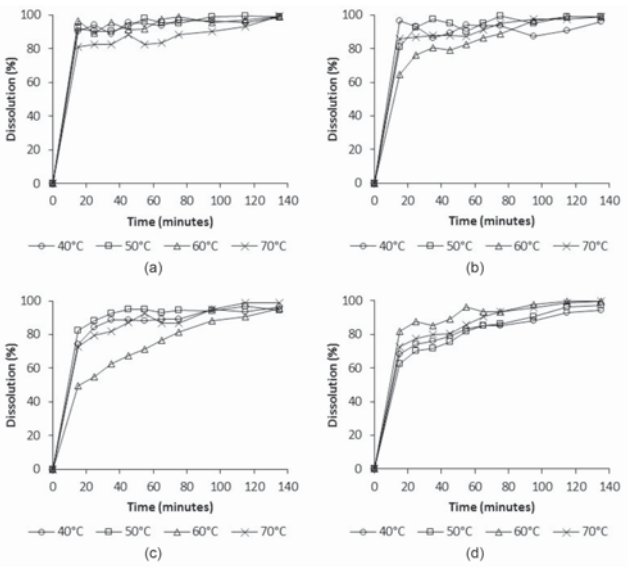

Figure 4—Effect of temperature on the rate of zinc leaching from zinc fume at (a) pH 1.2, (b) pH 1.5, (c) pH 1.8, and (d) pH 2.1

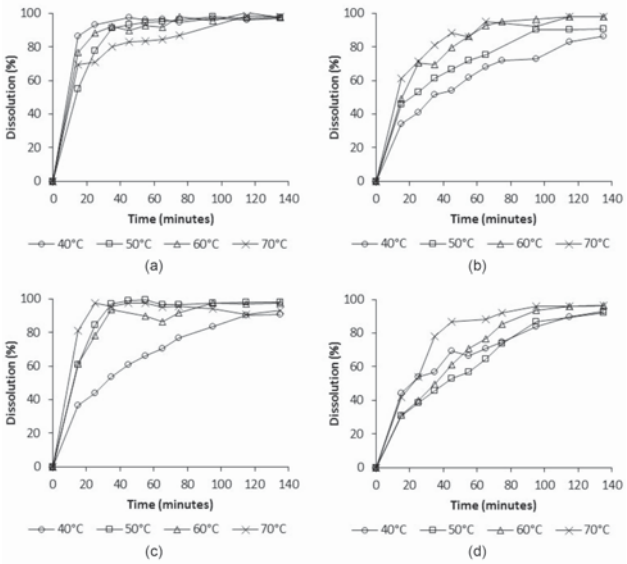

Figure 5—Effect of temperature on the rate of zinc leaching from zinc dross at (a) pH 1.2, (b) pH 1.5, (c) pH 1.8, and (d) pH 2.1

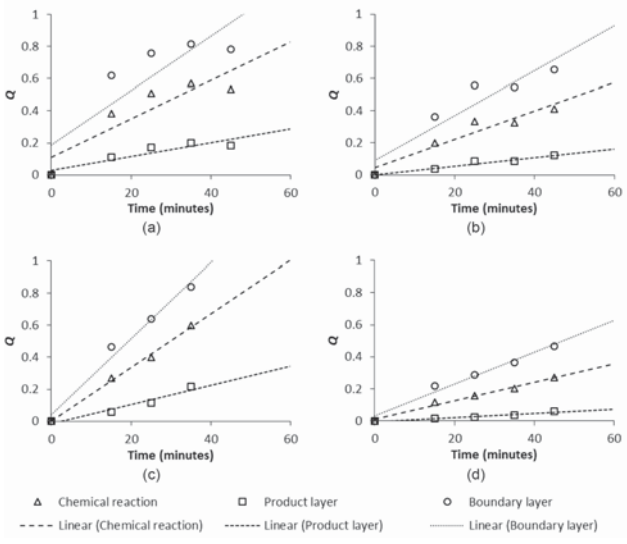

Figure 6—Comparison of consistency of rate limiting models with zinc leaching data from zinc dross tests performed at 60°C and (a) pH 1.2, (b) pH 1.5, (c) pH 1.8 ,and (d) pH2.1

Table III

Model parameters corresponding to the linear models shown in Figure 6

	Chemical reaction			Product layer			Boundary layer		
	k (min^{-1})	Intercept	R^2	*k* (min^{-1})	Intercept	R^2	*k* (min^{-1})	Intercept	R^2
pH 1.2	0.0119	0.113	0.79	0.0028	0.030	0.84	0.017	0.190	0.74
pH 1.5	0.0088	0.043	0.91	0.0027	0.001	0.94	0.014	0.088	0.88
pH 1.8	0.0167	0.003	0.99	0.0060	-0.014	0.95	0.024	0.041	0.98
pH 2.1	0.0058	0.011	0.99	0.0013	-0.005	0.94	0.010	0.029	0.98

A comparison of the overall zinc recovery at the expected plant residence time of 135 minutes for the different temperatures and pH conditions suggested that temperature had no statistically significant effect at pH 1.2. At higher pH values, the percentage zinc dissolution generally showed a slight increase with increasing temperature. Similarly, pH had a negligible effect on the extent of zinc leaching at 60°C and 70°C. At lower temperatures, the zinc dissolution decreased by up to 11 percentage points with an increase in pH to values of 1.5 or higher.

From Figure 7 it is evident that temperature and pH had no significant effect on zinc recovery from EAF dust after 135 minutes. These results suggest that the EAF dust identified as a potential alternative zinc oxide source for the Skorpion Zinc process contained a large proportion of readily leachable zinc oxide, with limited amounts of zinc ferrite. While the pH did not affect the leaching kinetics noticeably, the rate of zinc dissolution decreased when the temperature was increased above 60°C at all pH conditions investigated. This effect was observed only for leaching from EAF dust.

The elemental composition of the EAF dust and that of the zinc dross and the zinc fume differ in several respects. For example, the zinc content in EAF dust is low while the iron and impurity (Ca, Mn, and Mg) concentrations are high compared to the other materials. Given the comparative leaching rates at pH values between 1.2 and 2.1, and that the pH was controlled to the set-point value, it is unlikely that increased acid consumption by impurities at 70°C reduced the zinc leaching rate. It was, however, notable how the calcium leaching and precipitation behaviour varied for different sources and changed with temperature. No calcium precipitation was observed in the tests with fume dust, as the maximum achievable calcium concentration was below the calcium sulphate solubility limit. In the case of zinc dross, calcium precipitation did occur, but to a lesser extent than what was observed for EAF dust with the high calcium content. The calcium dissolution profiles for EAF dust at the different tests conditions are shown in Figure 8.

The average percentage calcium dissolution after 135 minutes decreased from 60% at 40°C to 47% at 70°C due to the decrease in calcium sulphate solubility with increasing temperature, as reported by Azimi, Papangelakis, and Dutrizac (2007). At 40°C and 50°C, fast initial calcium dissolution (up to 80%) was recorded at 15 minutes, followed by relatively rapid precipitation in the next 10 minutes and gradual or no further precipitation subsequently. The average drop in calcium concentration from 15 minutes to 135 minutes was 14.7 percentage points at 40°C and 18.4 percentage points at 50°C. At 60°C and 70°C, rapid precipitation is not observed because faster Ca dissolution and precipitation caused Ca to precipitate within the first 15 minutes of leaching. At 60°C, the drop in calcium

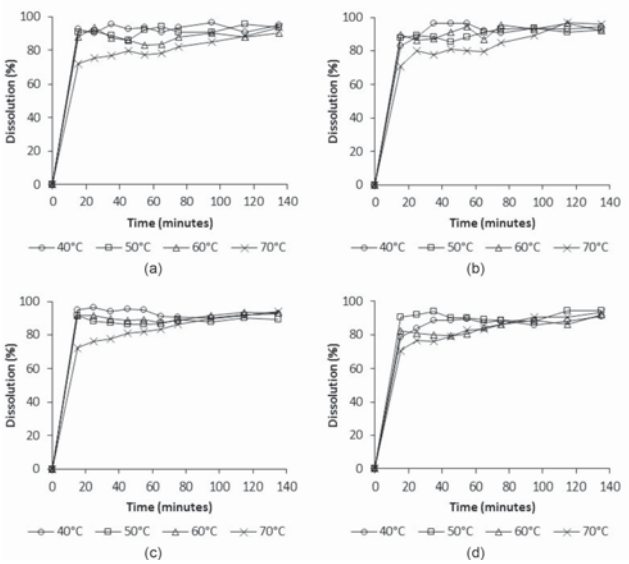

Figure 7—Effect of temperature on the rate of zinc leaching from EAF dust at (a) pH 1.2, (b) pH 1.5, (c) pH 1.8, and (d) pH 2.1

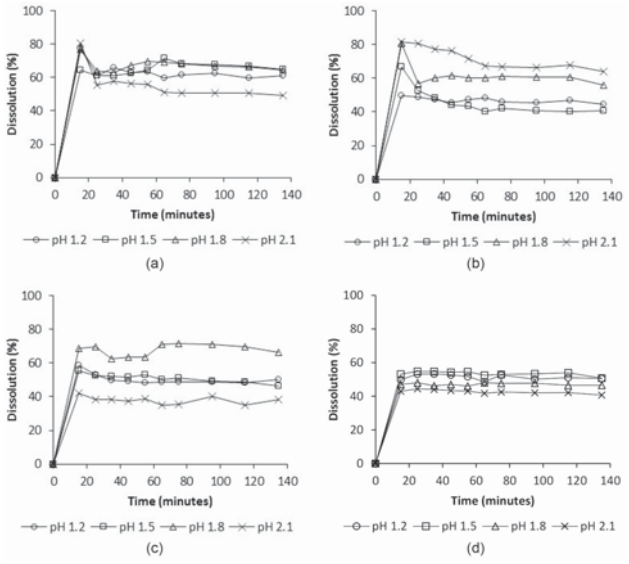

Figure 8—Effect of pH on the rate of calcium leaching from EAF dust at (a) 40°C, (b) 50°C, (c) 60°C, and (c) 70°C

concentration from 15 minutes to 35 minutes was 6 percentage points, while calcium precipitation was virtually complete within the first 15 minutes at 70°C.

These results suggest that the rates of calcium leaching and precipitation as calcium sulphate with increasing temperature became faster than the zinc leaching rate, resulting in partial passivation of the EAF dust particle surfaces. As a result, the extent of zinc dissolution decreased in the first 15 minutes of leaching and proceeded at a slow rate subsequently as mass transfer of reagents through the inert precipitate layer was required for the zinc leaching reactions to proceed. Decreased base metal leaching rates as a result of gypsum formation have also been reported by Gharabaghi, Irannajad, and Azadmehr (2013), who investigated nickel leaching from zinc plant residue, as well as Seidel and Zimmels (1998) and Seidel *et al.* (1999), who investigated aluminium leaching from coal fly ash. While increasing temperature is generally considered a requirement for faster leaching of zinc species such as zinc ferrite, it could possibly inhibit the leaching rate if the source contains calcium in sufficiently high concentrations to form significant amounts of calcium sulphate precipitate. The formation of a precipitate layer could also have contributed to the leaching behaviour observed for the fine particle size class, as discussed previously.

Aluminium and iron leaching

The effect of temperature on aluminium and iron dissolution from zinc fume did not show a clear trend. Dissolution in the pH range 1.2 to 1.5 was generally higher than in the range 1.8 to 2.1.The aluminium content of the zinc fume was an order of magnitude lower than that of the zinc dross and the EAF dust (Table I). The resulting aluminium concentration in the pregnant leach solution (PLS) was between 25 and 37 mg/L at the investigated conditions, which is below the acceptable limits for the Skorpion Zinc circuit. Similarly, the iron concentrations in the PLS between 160 and 260 ppm would typically be acceptable for the current Skorpion Zinc processing plant. The higher percentage iron leaching from zinc fume compared to EAF dust would therefore not be a problem given the relatively low iron content of the feed material.

In general, aluminium leaching from zinc dross increased with an increase in temperature, as shown in Figure 9. Aluminium dissolutions were 84.9% or higher at 60°C, and 88.9% or higher at 70°C in the pH range 1.2–1.8. The average aluminium dissolution of 88.9% at pH 1.2 was significantly higher than at the other pH conditions (between 65.4% and 67.4%). The effects of temperature and pH on aluminium leaching were similar to the effects observed for zinc leaching; this could be attributed to the presence of aluminium and zinc in similar forms in the dross. The trends observed for iron dissolution from zinc dross followed aluminium leaching closely, with high iron dissolution observed at pH 1.2 (88.6–94.0%) and at 60°C and 70°C in the pH range 1.2 to 1.8.

The 65% aluminium dissolution and 85% iron dissolution achieved at pH 1.8 and 50°C, which resemble typical current Skorpion Zinc operating conditions, might have a detrimental effect on downstream processing considering the relatively high impurity content of zinc dross. The resulting PLS had aluminium and iron concentrations in the range of 2.8–4.9 g/L and 1.4–2.4 g/L, respectively. The limitations that this places on the amount of dross that can be treated due to limited impurity removal capacity are investigated in more detail in part 2 of this communication.

The trends for aluminium dissolution from EAF dust were similar to those for zinc dross. The differences in percentage extraction were insignificant in the pH range 1.5 to 2.1, but the average aluminium dissolution of 67.3% at pH 1.2 was between 17 and 21 percentage points higher than at the other pH values. Although the greatest extent of aluminium dissolution in the pH range 1.5 to 2.1 occurred at the highest temperature, aluminium leaching appeared to be less sensitive to temperature at the lowest pH. Due to the lower percentage of aluminium leaching from, and lower aluminium content of, EAF dust compared to dross, the resulting PLS had a lower aluminium concentration, in the range 70–370 mg/L. From Figure 10 it can be seen that the extent of iron leaching from EAF dust was on average 45 and 27 percentage points lower than iron leaching from zinc dross and zinc fume, respectively. This was due mainly to presence of iron primarily in the form of iron oxides rather than zinc ferrite, which appeared to leach readily at the investigated conditions. The relatively low percentage iron dissolution and the presence of stable iron compounds also support the inhibition of zinc leaching due to entrapment of zinc species in insoluble iron phases. The iron content of the EAF dust was, however, more than five times higher than the iron content of the other materials. This resulted in relatively high iron concentrations in the PLS, ranging between 1.2 g/L and 8.3 g/L.

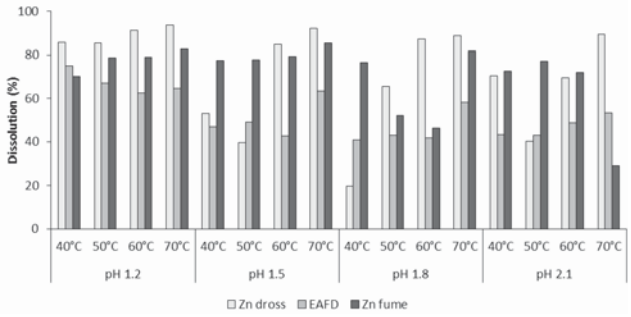

Figure 9—Percentage aluminium dissolution from the alternative zinc oxide sources after 135 minutes at different conditions

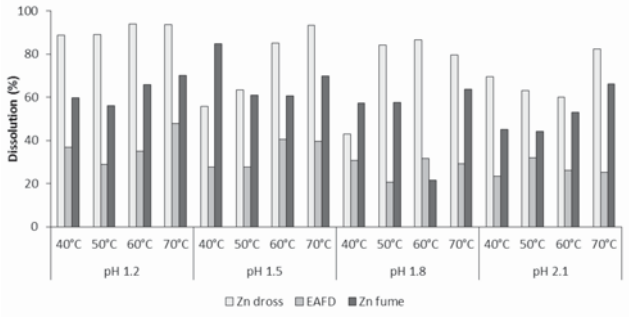

Figure 10—Percentage iron dissolution from the alternative zinc oxide sources after 135 minutes at different conditions

It is desirable to minimize iron extraction while maximizing zinc extraction, as iron may lead to overloading of the SX circuit and, ultimately, to the production of zinc that does not meet product specifications. In addition, leaching of iron instead of zinc leads to higher acid consumptions, which is a major focal point for cost optimization in any leaching process.

Acid consumption

Due to the significant contribution of acid to the operating costs of the Skorpion Zinc leaching plant, it was important to establish the acid consumptions of the potential secondary zinc oxide sources. The results reported here are for the base case, in which the normal Skorpion Zinc operating parameters were used (*i.e.* 50°C, pH 1.8, and 20% feed solids slurry). Figure 11a shows the total acid consumption in the leaching circuit alone, excluding acid consumed during filtration on the residue belt filters during the acid wash stage. EAF dust had the lowest leaching acid consumption at a total of 700 kg/t of feed, while the zinc dross had the highest consumption at 1380 kg/t of feed material. The acid consumption of zinc fume, at 1100 kg/t feed, was relatively low compared to the zinc dross due to the fact that it has the lowest impurity content. The relatively high zinc content did, however, result in a higher acid consumption than for EAF dust.

Evaluation of the gangue acid consumption for the alternative zinc oxide sources confirmed this interpretation of the acid consumption data. The gangue acid consumption was calculated based on the initial acid concentration, acid addition, residual acid concentration, and the stoichiometric amounts of acid required to achieve the specific extents of zinc dissolution. It is evident from Figure 11b that the zinc dross has the highest gangue acid consumption at a total of 540 kg/t of feed material, which contributed to the overall high leaching acid consumption for this material. As expected, the zinc fume, which had the lowest impurity content, had the lowest gangue acid consumption at 47 kg/t of feed.

Although the EAF dust contains the most impurities, it had a lower gangue acid consumption than the zinc dross, at a total of 330 kg/t of feed, because of the stability of the iron phases in EAF dust and the relatively low iron dissolution observed, as discussed previously.

Skorpion Zinc targets a gangue acid consumption of 150 kg/t for the ore to ensure that operating costs remain economically viable. Based on this target, only the zinc fume sample fell within the budgeted gangue acid consumption. However, since the zinc content in these samples is significantly higher than in the Skorpion Zinc ore, it may be possible to refine the samples economically regardless of the high acid consumption. To determine this, the total acid consumption for each source, including the acid consumed during re-acidification of the thickener underflow and during acid washing of the residue on the belt filters, was determined.

The targeted total overall acid consumption for the Skorpion Zinc ore is 1.5 t per ton of zinc. From Figure 12, it is clear that the acid consumption for all three oxide sources was lower than this target. The zinc dross and EAF dust had overall consumptions of 1.0 t and 1.3 t per ton Zn, respectively; the zinc fume acid consumption is the lowest of the three at 0.1 t per ton Zn. This is expected, as the gangue acid consumption is significantly lower for zinc fume (290 kg/t lower than for EAF dust), while the zinc content is approximately 78% compared to 30% for EAF dust and 60% for zinc dross. The zinc dross overall acid consumption per ton zinc is lower than that for EAF dust acid consumption, despite a higher gangue acid consumption, because it contains approximately double the amount of zinc.

Conclusions

A reduction in the particle size generally resulted in faster leaching kinetics due to the larger specific surface area, liberation of entrapped zinc species, and/or reduction in diffusion path lengths. A comparison of the recovery trends for the different samples revealed that the zinc fume yielded the highest overall zinc recovery of between 94.1 and 99.6%. The dissolution of zinc from zinc dross and EAF dust varied between 86.2 and 97.8% and 88.9 and 95.9%, respectively. Temperature did not have a significant effect on the extent of zinc leaching from the fume samples, but increasing the pH to 1.8 or higher at 40°C and 50°C did reduce the zinc leaching rate.

In the case of zinc dross, the rate of zinc dissolution also decreased with an increase in pH; the extent of zinc dissolution decreased by up to 11 percentage points when the pH was increased to 1.5 or higher. In the intermediate pH range, the leaching rate and extent of leaching increased with an increase in temperature. It was concluded that the rate-determining step for zinc leaching from dross gradually changed from mass transfer in a porous layer at pH 1.2 to chemical reaction and/or boundary-layer mass transport at higher pH values.

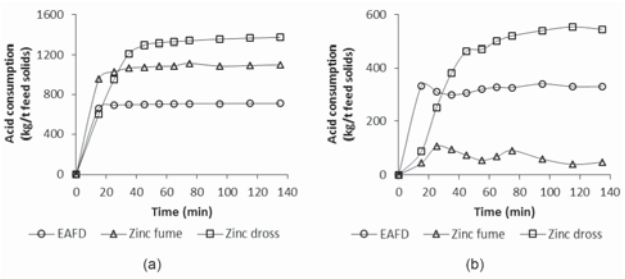

Figure 11—Comparison of (a) total acid consumption and (b) gangue acid consumption of the secondary oxides at the standard Skorpion Zinc operating conditions

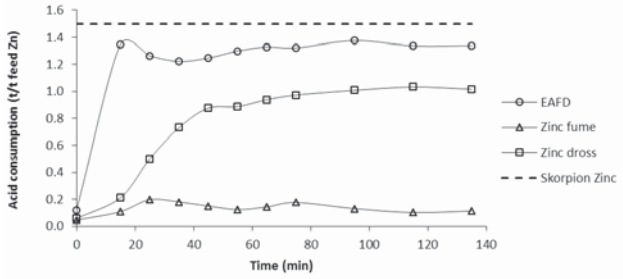

Figure 12 – Comparison of total acid consumption of the secondary oxides per unit mass of zinc at the standard Skorpion Zinc operating conditions

The EAF dust tested contained a high proportion readily leachable zinc species. Temperature had a significant effect on the zinc leaching rate only when increased to 70°C, at which point zinc leaching proceeded at a slower rate than at lower temperatures. This was due to the faster precipitation of calcium sulphate, which formed a passivating layer on the soluble zinc species and inhibited zinc dissolution.

Zinc dross reported the largest total and gangue acid consumptions of 1380 kg/t and 540 kg/t of feed material, respectively. Although EAF dust had a higher impurity content than zinc dross, the gangue acid consumption for EAF dust was lower than for zinc dross due to the presence of iron in sparingly soluble phases instead of easily soluble iron species. Iron dissolution from EAF dust varied between 20.7 and 47.7%, while 43.0–94.0% iron dissolved from dross. Given the high zinc and low impurity content of the zinc fume, more than 95% of the 1100 kg acid required per ton of feed material was utilized for zinc dissolution.

The gangue acid consumption was relatively high compared to the current Skorpion Zinc target of 150 kg acid per ton of feed material. However, the overall acid consumption for all three potential alternative zinc oxide sources was below the current Skorpion Zinc target of 1.5 t acid per ton of zinc in the feed material, due to the high zinc content of the alternative oxides compared to the ore.

Considering the leaching performance, it can be concluded that all three alternative zinc oxide sources could technically be used to supplement the ore feed to the Skorpion Zinc process at the current operating conditions. The optimal source and blending ratios have to be determined by mass balances and economic analyses, which are addressed in part 2 of this communication.

Acknowledgements

The authors gratefully acknowledge Skorpion Zinc for the supply of materials and financial support.

References

Azimi, G., Papangelakis, V.G., and Dutrizac, J.E. 2007. Modelling of calcium sulphate solubility in concentrated multi-component sulphate solutions. *Fluid Phase Equilibria*, vol. 260, no. 2. pp. 300–315. https://doi.org/10.1016/j.fluid.2007.07.069

Barrett, E.C., Nenniger, E.H., and Dziewinski, J. 1992. A hydrometallurgical process to treat carbon steel electric arc furnace dust. *Hydrometallurgy*, vol. 30, no. 1–3. pp. 59–68. https://doi.org/10.1016/0304-386X(92)90077-D

Behnajady, B., Babaeidehkordi, A., and Moghaddam, J. 2014. Determination of the optimum conditions for leaching of zinc cathode melting furnace slag in ammonium chloride media. *Metallurgical and Materials Transactions B: Process Metallurgy and Materials Processing Science*, vol. 45B. pp. 562–567. https://doi.org/10.1007/s11663-013-9971-0

Cruells, M., Roca, A., and Nunez, C. 1992. Electric arc furnace flue dusts: characterization and leaching with sulphuric acid. *Hydrometallurgy*, vol. 31, no. 3. pp. 213–231. https://doi.org/10.1016/0304-386X(92)90119-K

Dvořák, P. and Jandová, J. 2005. Hydrometallurgical recovery of zinc from hot dip galvanizing ash. *Hydrometallurgy*, vol. 77. pp. 29–33. https://doi.org/10.1016/j.hydromet.2004.10.007

Elgersma, F., Kamst, G.F., Witkamp, G.J., and van Rosmalen, G.M. 1992. Acidic dissolution of zinc ferrite. *Hydrometallurgy*, vol. 29, no. 1–3. pp. 173–189. https://doi.org/10.1016/0304-386X(92)90012-O

Gharabaghi, M., Irannajad, M., and Azadmehr, A.R. 2013. Leaching kinetics of nickel extraction from hazardous waste by sulphuric acid and optimization dissolution conditions. *Chemical Engineering Research and Design*, vol. 91, no. 2. pp. 325–331. https://doi.org/10.1016/j.cherd.2012.11.016

Gnoinski, J. 2007. Skorpion Zinc: optimisation and innovation. *Journal of the Southern African Institute of Mining and Metallurgy*, vol. 107. pp. 657–662.

Havlik, T., Friedrich, B., and Stopic, S. 2004. Pressure leaching of EAF dust with sulphuric acid. *Erzmetall*, vol. 57, no. 2. pp. 113–120.

Havlík, T., Souza, B.V. e, Bernardes, A.M., Schneider, I.A.H., and Miškufová, A. 2006. Hydrometallurgical processing of carbon steel EAF dust. *Journal of Hazardous Materials*, vol. B135. pp. 311–318. https://doi.org/10.1016/j.jhazmat.2005.11.067

Havlik, T., Turzakova, M., Stopic, S., and Friedrich, B. 2005. Atmospheric leaching of EAF dust with diluted sulphuric acid. *Hydrometallurgy*, vol. 77, no. 1–2. pp. 41–50. https://doi.org/10.1016/j.hydromet.2004.10.008

Herrero, D., Arias, P.L., Güemez, B., Barrio, V.L., Cambra, J.F., and Requies, J. 2010. Hydrometallurgical process development for the production of a zinc sulphate liquor suitable for electrowinning. *Minerals Engineering*, vol. 23, no. 6. pp. 511–517. https://doi.org/10.1016/j.mineng.2010.01.010

Hoang Trung, Z., Havlík, T., and Miškufová, A. 2015. . Processes for steelmaking dust treatment. https://www.researchgate.net/profile/Andrea_Miskufova/publication/228405625_PROCESSES_FOR_STEELMAKING_DUST_TREATMENT/links/54aed91e0cf29661a3d3aeab.pdf [accessed 30 May 2017].

Jandová, J., Prošek, T., and Maixner, J. 1999. Leaching of zinc oxide in aqueous sulphuric acid solutions. *Acta Metallurgica Slovaka*, 1999, no. 3. pp. 172–183. http://www.ams.tuke.sk/data/ams_online/1999/number3/mag02/mag02.pdf [accessed 30 May 2017].

Jha, M.K., Kumar, V., and Singh, R.J. 2001. Review of hydrometallurgical recovery of zinc from industrial wastes. *Resources, Conservation and Recycling*, vol. 33, no. 1. pp. 1–22. https://doi.org/10.1016/S0921-3449(00)00095-1

Kukurugya, F., Vindt, T., and Havlik, T. 2015. Behavior of zinc, iron and calcium from electric arc furnace (EAF) dust in hydrometallurgical processing in sulfuric acid solutions: Thermodynamic and kinetic aspects. *Hydrometallurgy*, vol. 154. pp. 20–32. https://doi.org/10.1016/j.hydromet.2015.03.008

Langová, Š., Riplová, J., and Vallová, S. 2007. Atmospheric leaching of steelmaking wastes and the precipitation of goethite from the ferric sulphate solution. *Hydrometallurgy*, vol. 87, no. 3–4. pp. 157–162. https://doi.org/10.1016/j.hydromet.2007.03.002

Li, Z. Q., Li, J., Zhang, L.B., Peng, J.H., Wang, S.X., Ma, A.Y., and Wang, B.B. 2015. Response surface optimization of process parameters for removal of F and Cl from zinc oxide fume by microwave roasting. *Transactions of Nonferrous Metals Society of China*, vol. 25, no. 3. pp. 973–980. https://doi.org/10.1016/S1003-6326(15)63687-1

Lottering, C. and Dorfling, C. 2018. Investigation of secondary zinc oxides as an alternative feed to the Skorpion Zinc process: Part 2 – Process considerations and economic analysis. *Journal of the Southern African Institute of Mining and Metallurgy*, vol. 118, no. 7. pp. 715–722.

Montenegro, V., Oustadakis, P., Tsakiridis, P.E., and Agatzini-Leonardou, S. 2013. Hydrometallurgical treatment of steelmaking electric arc furnace dusts (EAFD). *Metallurgical and Materials Transactions B: Process Metallurgy and Materials Processing Science*, vol. 44, no. 5. pp. 1058–1069. https://doi.org/10.1007/s11663-013-9874-0

Moradi, S. and Monhemius, A.J. 2011. Mixed sulphide-oxide lead and zinc ores: Problems and solutions. *Minerals Engineering*, vol. 24, no. 10. pp. 1062–1076. https://doi.org/10.1016/j.mineng.2011.05.014

Oustadakis, P., Tsakiridis, P.E., Katsiapi, A., and Agatzini-Leonardou, S. 2010. Hydrometallurgical process for zinc recovery from electric arc furnace dust (EAFD). Part I: Characterization and leaching by diluted sulphuric acid. *Journal of Hazardous Materials*, vol. 179, no. 1–3. pp. 1–7. https://doi.org/10.1016/j.jhazmat.2010.01.059

Pecina, T., Franco, T., Castillo, P., and Orrantia, E. 2008. Leaching of a zinc concentrate in H_2SO_4 solutions containing H_2O_2 and complexing agents. *Minerals Engineering*, vol. 21, no. 1. pp. 23–30. https://doi.org/10.1016/j.mineng.2007.07.006

Pereira, C.F., Galiano, Y.L., Rodríguez-Piñero, M.A., and Parapar, J.V. 2007. Long and short-term performance of a stabilized/solidified electric arc furnace dust. *Journal of Hazardous Materials*, vol. 148, no. 3. pp. 701–707. https://doi.org/10.1016/j.jhazmat.2007.03.034

Prosser, A.P. 1996. Review of uncertainty in the collection and interpretation of leaching data. *Hydrometallurgy*, vol. 41, no. 2–3. pp. 119–153. https://doi.org/10.1016/0304-386X(95)00071-N

Rabah, M.A., and El-Sayed, A.S. 1995. Recovery of zinc and some of its valuable salts from secondary resources and wastes. *Hydrometallurgy*, vol. 37, no. 1. pp. 23–32. https://doi.org/10.1016/0304-386X(94)00015-U

Ruşen, A., Sunkar, A.S., and Topkaya, Y.A. 2008. Zinc and lead extraction from Çinkur leach residues by using hydrometallurgical method. *Hydrometallurgy*, vol. 93, no. 1–2. pp. 45–50. https://doi.org/10.1016/j.hydromet.2008.02.018

Seidel, A., Sluszny, A., Shelef, G., and Zimmels, Y. 1999. Self inhibition of aluminum leaching from coal fly ash by sulfuric acid. *Chemical Engineering Journal*, vol. 72, no. 3. pp. 195–207. https://doi.org/10.1016/S1385-8947(99)00006-6

Seidel, A., and Zimmels, Y. 1998. Mechanism and kinetics of aluminum and iron leaching from coal fly ash by sulfuric acid. *Chemical Engineering Science*, vol. 53, no. 22. pp. 3835–3852. https://doi.org/10.1016/S0009-2509(98)00201-2

Shawabkeh, R.A. 2010. Hydrometallurgical extraction of zinc from Jordanian electric arc furnace dust. *Hydrometallurgy*, vol. 104, no. 1. pp. 61–65. https://doi.org/10.1016/j.hydromet.2010.04.014

Shitov, A.V, Klimushkin, A.N., Stolyarskii, O.A., and Agapeev, E.N. 2005. Recycling of the dross formed in hot galvanizing. *Metallurgist*, vol. 49, no. 7–8. pp. 296–298.

Trpčevská, J., Hluchá ová, B., Vindt, T., Zorawski, W., and Jakubéczyová, D. 2010. Characterization of the bottom dross formed during batch hot-dip galvanizing and its refining. *Acta Metallurgica Slovaca*, vol. 16, no. 3. pp. 151–156. https://doi.org/10.1007/s13398-014-0173-7.2

Turan, M.D., Altundo an, H.S., and Tümen, F. 2004. Recovery of zinc and lead from zinc plant residue. *Hydrometallurgy*, vol. 75. pp. 169–176. https://doi.org/10.1016/j.hydromet.2004.07.008 ◆